Proceedings of the Korean Nuclear Society Spring Meeting
Kori, Korea, May 2000

In-Reactor Corrosion Test for Modern Cladding Materials (IFA-638)

Yong-Deog Kim

Korea Electric Power Research Institute
103-16 Munji-dong, Yusung-gu
Taejeon, Korea 305-380

ABSTRACT

A cladding corrosion test (IFA-638) is being conducted at the Halden Project with the main objective to investigate the corrosion behaviour of modern PWR cladding materials at increasing burnup/neutron fluence under PWR conditions. There are two parts to the experiment. one using fuelled cladding sections and the other using unfuelled coupons made from quarter and one-third sectors of cladding. The materials being studied as fuelled sections are low tin Zr-2 and Zr-4, high tin Zr-4, ZIRLO, M4 and M5 and Alloy A and E635. Thirty-six (36) cladding coupons have been prepared from the cladding materials provided by ABB-Atom, Framatome and Mitsubishi Heavy Industries. This report summarizes the operating conditions during the second irradiation period and the results of the first and second interim inspections. Interim inspections were carried to assess the oxide growth of both the fuel cladding and the coupons during the shutdown. The eddy current technique was used on the fuel rods and the coupons were weighed and visually examined.

1. INTRODUCTION

Zircaloy corrosion was formerly not considered a limiting factor for commercial PWR reactor operation. However, the operational conditions for advanced nuclear power reactors , both PWR and BWR, have become more demanding (higher burnup and power density levels) in order to increase uranium utilization and to minimize the amount of spent fuel storage. The waterside corrosion and hydriding of Zircaloy cladding is considerably accelerated at increased

discharge burnup levels beyond 50-60 MWd/kg U, and has become a possible life-limiting factor which has resulted in a need for improved Zircaloy cladding materials. Therefore. several different zirconium based alloys were developed with the intention of improving cladding corrosion resistance. Design criteria must also make allowance for loss of ductility with time (fluence) and the degradation of heat transfer conditions owing to the buildup of corrosion film and crud. Work is also underway to investigate corrosion (irradiation damage, H_2 pickup) enhancement factors due to irradiation.

The need for improved Zircaloy cladding materials has been addressed by two parallel approaches, improvements to Zirealoy-4 and the development of new alloy compositions. The new PWR cladding corrosion rig, IFA 638 was loaded in late June 1998 with the aim of studying the corrosion behaviour of different modern Zircaloy cladding materials at increased discharge burnup levels. The materials were provided by the four organisations: ABB-Atom, ENUSA, Framatome and Mitsubishi Heavy Industries. There are two parts to the experiment, one using fuelled cladding sections and the other using unfuelled coupons made from quarter or third sectors of cladding. The materials being studied as fuelled sections are low tin Zr-2 and Zr-4, high tin Zr-4, ZIRLO, M4 and M5 and Alloy A and E635. A combination of fresh and pre-irradiated cladding is being used which will allow the effect of fluence on the corrosion behaviour to be studied. Thirty-six (36) cladding coupons have been prepared from cladding materials supplied by ABB-Atom, Framatome and Mitsubishi Heavy Industries.

This report presents the experimental conditions for the test rig IFA-638, and the first and second interim inspection results and the oxide growth data of the different materials are discussed.

2, DESCRIPTION OF THE EXPERIMENT

2.1 Rig and loop

A schematic representation of the test rig is shown in Figure 1. The rig is of the fuelled flask assembly design with three test rods (section 2.2) contained within the pressure flask. Attached to the top of each fuel rod is a coupon holder, which can hold up to a total of 7-8 coupons in an upper and lower position. There is also a central coupon holder that runs along the length of the fuel rods, which has 15 positions of which 13 were used in the first irradiation cycle. Thirty-six (36) unfuelled cladding coupons (section 2.3) were contained in the test rig. Thermocouples are placed at the inlet and outlet of the test section to monitor the coolant conditions. Three vanadium neutron detectors are distributed vertically within the pressure flask in order to determine the axial flux and power distribution. Representative fast neutron

flux conditions are created by the booster rods which have a relatively high enrichment of 13-wt%, and are cooled by heavy water under forced circulation and HBWR conditions (24 bar, 2400C and 0.9 m/s). They span from 700 to 1500 mm above the reactor core plate, thus covering both the test rods and the coupons.

2.2 Fuelled cladding sections

Three fuelled test rods were installed in IFA-638. Each test rod of fuelled cladding is composed of four segments prepared from a combination of fresh and pre-irradiated materials provided by ABB-Atom, ENUSA and Framatome, as shown in Figure 2 and summarised in Table 1. Each segment comprises approximately 120 mm of cladding material with an O.D. of 9.5 mm and I.D. of either 8.36, 8.30 or 8.25 mm. The six segments of the pre-irradiated materials were mechanically defuelled, and filled with 8 wt% U-235 enriched UO_2 pellets to an active fuel stack length of 90 mm. For each test rod the bottom two segments are fresh cladding material while the upper two are pre-irradiated claddings (see Figure 2).

2.3 Unfuelled coupons

The test rig includes thirty-six (36) unfuelled cladding coupons. The cladding coupons have been prepared from cladding materials provided by ABB-Atom, Framatome and Mitsubishi Heavy Industries. The test matrix and individual positioning of each coupon in the test rig are outlined in Table 2.

2.4 Operating conditions

This rig has been operated from the start-up in June 1998 until the end of Setember 1999. During the course of irradiation a total of 263 FPD was accumulated and an assembly burnup of 11.9 MWd/kgUO2 was achieved. Examples of the measured neutron flux levels and the axial neutron flux profiles in the in-core section of the rig are shown in Figures 3. The relative positions of the fuelled cladding rods and the booster rods in the core are also presented in the figures. Figure 4 shows the history of inlet and outlet temperature and pressure for the entire irradiation cycle. The coolant outlet and inlet temperature and the pressure in the rig were kept at about 317 ℃, 310 ℃, and 159 bar, respectively, while the inlet flow rate was maintained at 1.8 m/s. The average linear heat rate (A.LHR) for the test assembly was about 32 kW/m in IFA-638.1 and between 27 and 21 kW/m during operation of IFA-628.2 and 3 (see Figure 5). The main operating conditions for IFA-638.1 to 3 are summarised in Table 3. Fast neutron flux also shown in Table 3 are the calculated average fast neutron flux within the fuel rod region and immediately above each of the test rods. During irradiation, the concentration of boron and lithium were monitored frequently and maintained at about 1000 and 3 ppm, respectively,

corresponding to a calculated pH300-value of between 7.08 and 7.16. The concentration of hydrogen was maintained in the range of 2-4 ppm, as specified.

2.5 Interim inspections

During the end-of-year shutdown (December 1998 - December 1999), interim inspections were carried out to assess the oxide growth of both the fuel cladding and the coupons. Following visual examination, the eddy current technique was used to measure the oxide thickness on the fuel rods, and the coupons were weighed.

2.5.1 Fuelled cladding sections

Axial oxide thickness profiles were measured on the fuelled cladding sections. The rods were unloaded from the rig and transferred to the handling compartment where they were mounted in a special inspection rig allowing an axial movement of the rod while registering the layer thickness by means of an Eddy Current (EC) proximity probe. According to the manufacturer of the EC equipment, the accuracy of the measurements is empirically estimated to be within 2 gm.

Measurements of the oxide thickness along the pre-irradiated fuelled cladding sections were also carried out prior to loading of the rig in the reactor. Seven axial traces were obtained for the pre-irradiated segments at six angular orientations (0 ° / 360 ° , 60 ° , 120 ° , 180 ° , 240 ° , 300 °) where the orientation 0 ° faces to the centre of the rig and 180 ° to the outside, respectively. After irradiation period, EC-measurements were performed for all rods at the same angular orientations. Moreover, the fresh cladding material sections were brushed to remove possible traces of crud. After brushing, the oxide layer thickness of the fresh cladding material sections was measured at two angular orientations (0 ° /360 ° , 180 °).

Since the test materials comprise several different zirconium based alloys, individual calibration of the EC-proximity probe was undertaken for each alloy using, as reference, unirradiated segments of the respective canning materials.

2.5.2 Unfuelled coupons

All the coupons were weighed before irradiation. After irradiation, the coupons were removed from the coupon holders, washed and weighed in the compartment on a five point balance.

3. EXPERIMIENTAL OBERVATIONS

The more demanding PWR fuel duties have necessitated improvements in the cladding

corrosion resistance particularly at burn-ups exceeding 40-50 MWd/kgU. The test matrix and configuration of IFA 638 has created an unique possibility to investigate and compare the corrosion behaviour of different modern Zr based cladding materials simultaneously as influenced by temperature, heat rate and fast neutron flux.

The use of unfuelled coupons, in addition to fuelled pre-irradiated and fresh cladding sections, enables evaluation of effects of heat rate and neutron flux on the degradation of the cladding materials at increasing burnup/neutron fluence.

A summary of the results and observations after the first and second interim inspection are presented in the following two chapters.

3.1 Unfuelled coupons

Weight gain (mg/dm^2) measurements for all the coupons were carried out to assess the oxide growth of the coupons in the first interim inspection after 125 and 263 FPD of irradiation.

The weight gain [mg/dm^2] for the coupons are summarised in Table 4.

3.2 Fuelled cladding sections

ABB Atom, Framatome and ENUSA have supplied the cladding materials for the three test rods which were fuelled with fresh 8 wt% U-235 enrichment UO_2 pellets. The three fuel rods were prepared from Zr-2 (low-Sn), Zr-4 (high-Sn), Zr-4 (low Sn), ZIRLO, Alloy E635, Alloy A, M4 and M5. as shown in Figure 2. Visual inspection of Alloy E635, Alloy A, M4 and M5 showed uniform black cladding surfaces, while Zr-2 (low Sn), Zr-4 (high Sn) and the ZIRLO cladding revealed an oxide surface with a more patchy appearance.

The results of the measurements on the materials are summarised in Table 5.

4. SUMMARY

The test matrix and experimental configuration of IFA 638 enables the corrosion properties of many materials to be studied simultaneously as influenced by temperature, heat flux and neutron flux. Some of the main observations were as follows

1. An increase in oxide thickness ranging from ~ 4 to ~ 8 µm were determined on the pre-irradiated fuelled cladding sections, while increases ranging from ~ 6 to ~ 9 µm were measured on the fuelled, initially fresh, cladding segments. The results imply that the corrosion rate of the different Zr based cladding materials may be less sensitive to irradiation than conventional materials. (A greater influence of positive temperature feedback leading to

a self-acceleration of the corrosion. might have been expected).

2. The results of the weighing of the coupons showed values ranging from 15 to 44 gm after second interim inspection.

3. The corrosion rates of the as-received M4 and M5 coupons, supplied by Framatome, it appears that M4 and in particular M5 may have improved corrosion resistance.

4. It is once again pointed out that the data presented in this HWR report are based on only two cycles of irradiation and observations must be considered preliminary, since long term irradiation and further interim inspections are necessary to analyse trends in irradiation sensitivity, possible enhancement factors at burn-ups exceeding 40-50 MWd/kg U, and to obtain a consistent relative comparison of the different materials.

5. The intention of the IFA 638 corrosion test rig is to operate it over a long period of time (3-4 years) to a burnup of about 50 MWd/kg UO_2. The progress of corrosion will be determined during regular interim inspections, and the test rods and coupons can be exchanged such that other materials can be introduced at any time, should this be desired.

5. ACKNOWLEDGMENTS

A number of persons have contributed to this corrosion test. The authors wish to express their gratitude to T. Johnsen and K.W. Eriksen for performing the oxide measurements during the interim inspection, P. Gunnerud for loop operation, N.S. Normann, T.J. Lindskog and T.K. Solheim for water chemistry control and analysis, and Fuel Division Staff at the Project for useful advise.

6. REFERENCES

1. T.Tsukada, T.Johnsen, P.Gunnerud. K.Fjellestad, C.Vitanza, "Analysis of the Water Corrosion Experiment in IFA-560.2", HWR-236, 1988.

2. T.Kido and K.Ranta~Ruska, "Zircaloy Corrosion at High LIOH Concentration under PWR Conditions (IFA-568.1 Final Report)", HWR-333,1992.

3. M.A.MeGrath and D.Deuble, "The PWR Corrosion Test IFA-593.2-4: Irradiation Data, Observations and Modelling Aspects", HWR-533, 1998.

4. M.Nakata and E.Hauso, "Summary of Characterisation Data on Cladding Materials Used in the Corrosion Test IFA-638 and in the Creep Test IFA-617", HWR-566, 1998.

5. F.Garzarolli, D.Jorde, R.Manzel, G.W.Parry, P.G.Smerd,"Review of PWR Fuel Rod Water-side Corrosion Behavior',EPRI-NP-1472. 1980.

6. A.Frichet, H. Amanrich, "Irradiation effects on corrosion behaviour of different zirconium base alloys", Enlarged HPG Meeting at Lillehammer, March 1998.

7. T.M.kido,”A study on Enhanced Uniform Corrosion of Zirealoy-4 cladding during high burnup operation in PWRs", Sixth International Symposium on Environmental Degradation of Materials on Nuclear Power System-Water Reactors, 1993.

8. E.Kolstad, T.M.Karlsen, "Summary of Workshop Meeting on Zircaloy Corrosion and Hydriding" 5HWR-367,1994.

9. M.Limback, M.A.Krammen, P.Rudling, S.R.Pati and A.M.Garde, "Corrosion and Hydriding Performance of Zirealoy-2 and Zircaloy-4 Cladding Materials in PWRS", Proceedings of the ANS International Topical Meeting on Light Water Reactor Fuel Performance, West Pal Beach, Florida, April 1994, pp.286-295.

10. A.V.Antonina et al., "Zirconium Alloy E635 as a Material for Fuel Rod Cladding and Other Components of VVER and RBMK Cores", Zirconium in the nuclear industry: Eleventh International Symposium, ASTM STP 1295, 1996, pp. 785-804.

11. M.Limb'a'ck, "A Brief Overview of Some of the Commercially Available Zirconium Based Alloys", F-Note 1349, January 1996.

12. J.P.Mardon, G.Garner, P.Beslu, D.Charquet, J.Senevat, 'Update on the development of advanced zirconium alloys for PWR fuel rod claddings" International Topical Meeting on Light Water Reactor Fuel Performance, Portland, March 1997.

13. T.J.Bjorlo, E.Kolstad, C.Vitanza, 'Fuel Temp-2, A Computer Programme for Analyzing the Steady State Thermal Behaviour of Oxide Fuel Rods', HRP-211, 1977.

14. R.J.White, "Modifications to the FTEMP-2 Fuel Temperature Calculation Code", F-Note 1430, October 1997.

15. G.P.Sabol, R.J.Comstock et al., "In-Reactor Corrosion Performance of ZIRLO and Zircaloy-4", Zirconium in the nuclear industry: Tenth International Symposium, ASTM STP 1245, 1994, pp. 724-744.

16. Magnus Limb'a'ck, 'Comparison of Models For Zircaloy Cladding Corrosion in PWRS", HWR 468, March 1996.

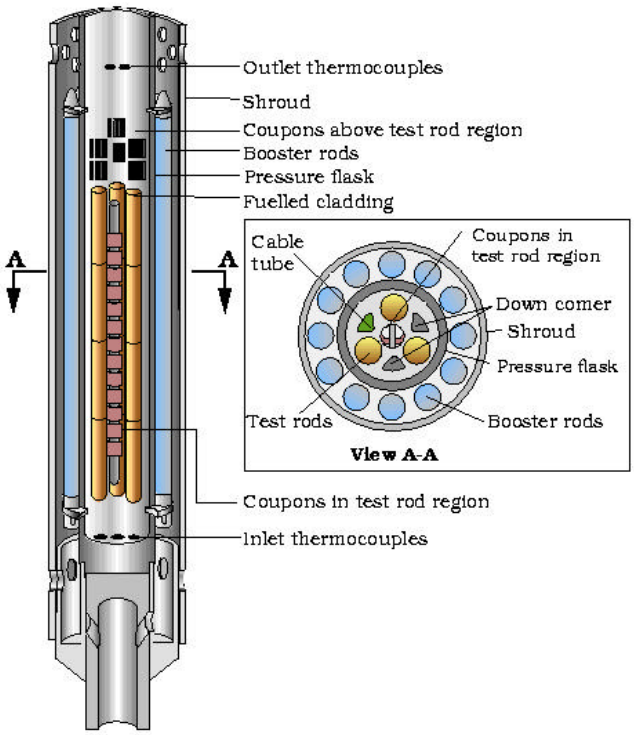

Figure 1. Lay-out of the PWR cladding corrosion rig, IFA 638

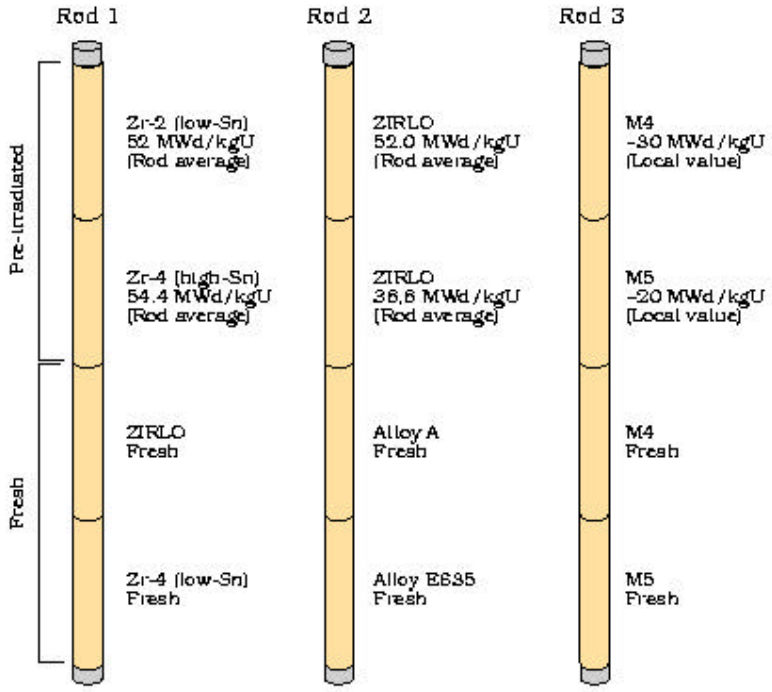

Figure 2. Schematic lay-out of the fuel rods used in the PWR cladding corrosion test, IFA-638.

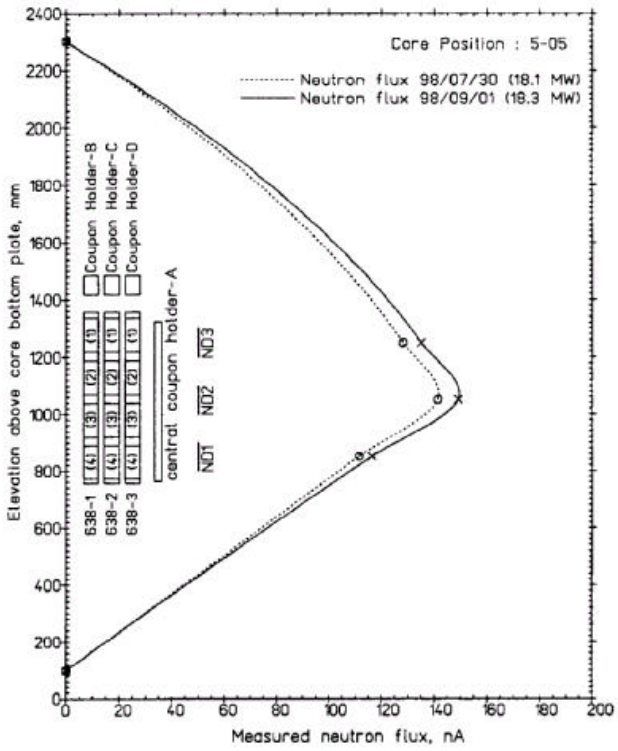

Figure 3. Axial positions of fuelled sections and coupons and neutron flux profile of IFA-638.

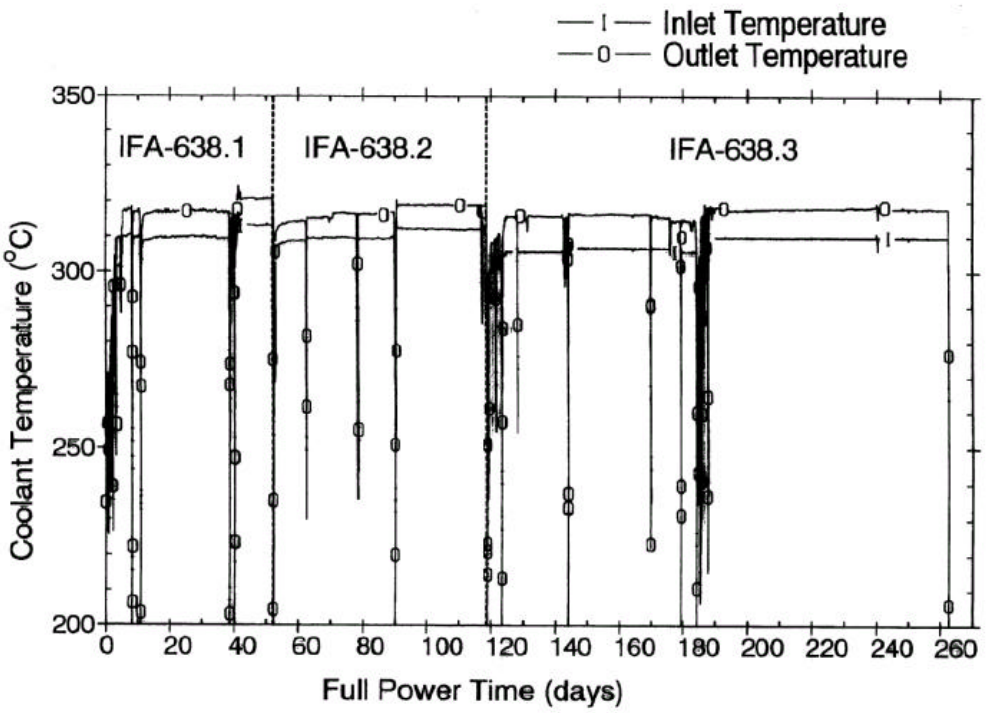

Figure 4. Coolant inlet and outlet temperature of IFA-638.1–3.

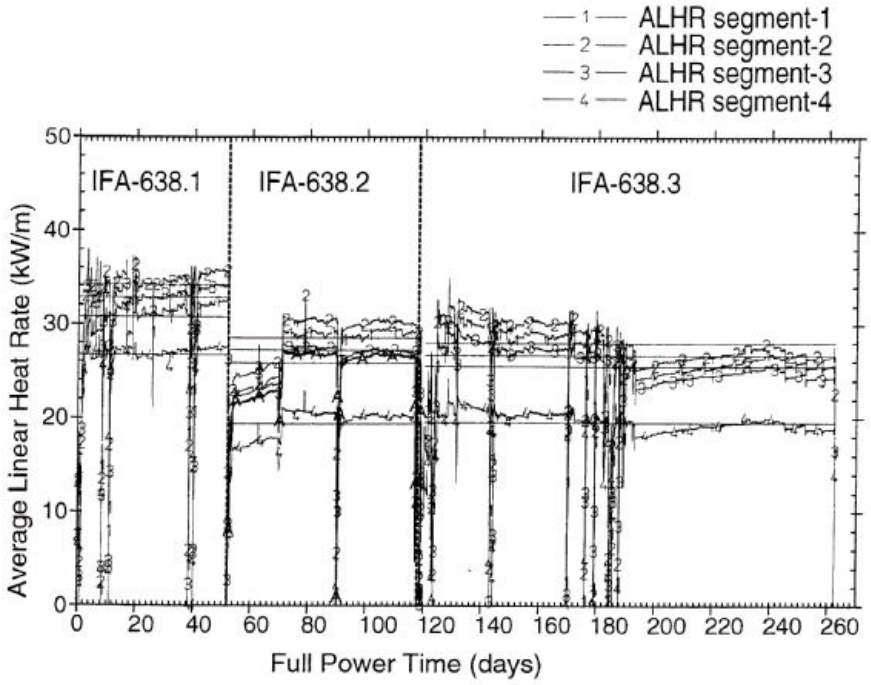

ALHR1: 30.707	ALHR1: 27.207	ALHR1: 26.719
ALHR2: 34.155	ALHR2: 28.559	ALHR2: 27.943
ALHR3: 32.849	ALHR3: 25.836	ALHR3: 25.475
ALHR4: 26.766	ALHR4: 19.360	ALHR4: 19.487

Figure 5. Power history of the fuelled section.

Table 1. Test Matrix of Fuelled Cladding Section.

Rod No. (Segment No.)	Materials	Segment Burnup [MWd/kgU]	Rod Average Burnup [MWd/kgU]	Initial Average Oxide-thickness [mm]	Supplier
638-1 (1)	Zr-2 (low-Sn)	~ 32	52.0	22.8	ABB-Atom
638-1 (2)	Zr-4 (high-Sn)	~ 34	54.4	31.3	ABB-Atom
638-1 (3)	ZIRLO	Fresh	Fresh	--	ENUSA
638-1 (4)	Zr-4 (low-Sn)	Fresh	Fresh	--	ENUSA
638-2 (1)	ZIRLO	~ 32	52.0	20.7	ABB-Atom
638-2 (2)	ZIRLO	~ 22	~ 36.6	14.7	ABB-Atom
638-2 (3)	Alloy A	Fresh	Fresh	--	ABB-Atom
638-2 (4)	Alloy E635	Fresh	Fresh	--	ABB-Atom
638-3 (1)	M4	~ 30	~ 39	19.5	Framatome
638-3 (2)	M5	~ 20	~ 28	15.3	Framatome
638-3 (3)	M4	Fresh	Fresh	--	Framatome
638-3 (4)	M5	Fresh	Fresh	--	Framatome

Holder Position I.D.	Channel Pos.	Material	Supplier
In the test rod region, axial extent 762 - 1324 mm			
A1	A.1	MDA-S	MHI
A2	A.2	MDA-H	MHI
A3	A.3	MDA-R	MHI
A4	A.4	MDA-L	MHI
A5	A.5	MDA-S	MHI
A6	A.6	MDA-H	MHI
A7	A.7	MDA-R	MHI
A8	A.8	MDA-L	MHI
A9	A.9	MDA-S	MHI
A10	A.10	MDA-H	MHI
A11	A.11	MDA-R	MHI
A12	A.12	MDA-L	MHI
A13	A.13	SRA Low-Sn Zr-4	ABB-Atom
A14	A.14	EMPTY	
A15	A.15	EMPTY	
Above test rod number 638-1, axial extent 1455 - 1485 mm			
B1 (Upper)	B.1.1	SRA Low-Sn Zr-2	ABB-Atom
B1 (Upper)	B.1.2	SRA High-Sn Zr-4	ABB-Atom
B1 (Upper)	B.1.3	Alloy A	ABB-Atom
B1 (Upper)	B.1.4	Alloy E635	ABB-Atom
Above test rod number 638-1, axial extent 1417 - 1447 mm			
B2 (Lower)	B.2.1	Zr-4 AFA 2G (AFA)	Framatome
B2 (Lower)	B.2.2	Zr-4 AFA 2G (A31)	Framatome
B2 (Lower)	B.2.3	Zr-4 AFA 2G (AA)	Framatome
B2 (Lower)	B.2.4	Zr-4 AFA 2G (A43)	Framatome
Above test rod number 638-2, axial extent 1455 - 1485 mm			
C1 (Upper)	C.1.1	SRA Low-Sn Zr-4	ABB-Atom
C1 (Upper)	C.1.2	PRXA Low-Sn Zr-4	ABB-Atom
C1 (Upper)	C.1.3	M5 (M5)	Framatome
C1 (Upper)	C.1.4	Zr-4 AFA 2G (- -)	Framatome
Above test rod number 638-2, axial extent 1417 - 1447 mm			
C2 (Lower	C.2.1	RXA Zr-4 (GTT)	ABB-Atom
C2 (Lower)	C.2.2	RXA Zr-4 (GTT)	ABB-Atom
C2 (Lower)	C.2.3	M5 (MA)	Framatome
Above test rod number 638-3, axial extent 1455 - 1485 mm			
D1 (Upper)	D.1.1	Alloy B	ABB-Atom
D1 (Upper)	D.1.2	Alloy C	ABB-Atom
D1 (Upper)	D.1.3	SRA Sandvik Alloy	ABB-Atom
D1 (Upper)	D.1.4	RXA Sandvik Alloy	ABB-Atom
Above test rod number 638-3, axial extent 1417 - 1447 mm			
D2 (Lower)	D.2.1	M4 (M4)	Framatome
D2 (Lower)	D.2.2	M4 (RA)	Framatome
D2 (Lower)	D.2.3	M4 (R28)	Framatome
D2 (Lower)	D.2.4	M5 (M26)	Framatome

Table 2. Test Matrix of Unfuelled Coupons in IFA-638.

Table 3. Summary of Operational Conditions.

IFA 638	638-1	638-2	638-3 (I)	638-3 (II)
Number of FPD	52	66	66	78
ALHR upper part (kW/m) ALHR lowest part (kW/m)	31 - 34 ~ 27	26 - 29 ~ 19	28 - 30 ~ 21	25 - 27 ~ 18
Average coolant temperature (°C)	~ 310 (inlet) ~ 317 (outlet)		~ 306 (inlet) ~ 315 (outlet)	~ 309 (inlet) ~ 318 (outlet)
Rig pressure (bar)	~ 159		~ 158	
Inlet velocity (m/s)	1.9		1.2	
Water chemistry: Lithium (ppm) Boron (ppm) pH_{300}	 2.7 - 3.3 953 - 1030 ~ 7.1	 2.8 - 3.3 988 - 1039 ~ 7.1	 2.8 - 3.3 994 - 1035 ~ 7.1	

Table 4. The Second Interim Inspection results of Unfuelled Coupons in IFA-638.

coupon No.	Material	initial data [mg]	2nd Inerim Inspection [mg]	Weight Gain [mg]	Weight Gain [mg/dm²]	OD(dm)	ID(dm)	Length(dm)	Surface area [dm²]	Oxide-layer thickness [mm]
A1	MDA-S	723.4	725.81	2.41	54.98	0.095	0.0836	0.3	0.04383	3.8
A2	MDA-H	718.4	720.76	2.36	53.84	0.095	0.0836	0.3	0.04383	3.7
A3	MDA-R	727.1	729.43	2.33	53.16	0.095	0.0836	0.3	0.04383	3.6
A4	MDA-L	708.6	711.02	2.42	55.21	0.095	0.0836	0.3	0.04383	3.8
A5	MDA-S	730	732.32	2.32	52.93	0.095	0.0836	0.3	0.04383	3.6
A6	MDA-H	714.8	716.95	2.15	49.05	0.095	0.0836	0.3	0.04383	3.4
A7	MDA-R	717.1	719.2	2.1	47.91	0.095	0.0836	0.3	0.04383	3.3
A8	MDA-L	715.1	717.29	2.19	49.96	0.095	0.0836	0.3	0.04383	3.4
A9	MDA-S	730.5	732.63	2.13	48.59	0.095	0.0836	0.3	0.04383	3.3
A10	MDA-H	723.3	725.27	1.97	44.94	0.095	0.0836	0.3	0.04383	3.1
A11	MDA-R	707.7	709.68	1.98	45.17	0.095	0.0836	0.3	0.04383	3.1
A12	MDA-L	729.1	731.2	2.1	47.91	0.095	0.0836	0.3	0.04383	3.3
A13	SRA Low-Sn Zr-4	726.9	728.84	1.94	44.26	0.095	0.0836	0.3	0.04383	3
A14*	WWER(Zr-1%Nb)	859.23	859.98	0.75	17.11	0.095	0.0836	0.3	0.04383	1.2
A15*	Standard Zr-4 (high Sn)	726.24	727.39	1.15	26.24	0.095	0.0836	0.3	0.04383	1.8
B1-1	SRA Low-Sn Zr-2	985.3	988.06	2.76	47.48	0.095	0.0836	0.3	0.05813	3.2
B1-2	SRA High-Sn Zr-4	991.1	993.98	2.88	49.55	0.095	0.0836	0.3	0.05813	3.4
B1-3	Alloy A	961.8	964.24	2.44	41.98	0.095	0.0836	0.3	0.05813	2.9
B1-4	Alloy E635	992.6	995.31	2.71	46.62	0.095	0.0836	0.3	0.05813	3.2
B2-1	Zr-4 AFA2G (AFA)	939	941.37	2.37	40.77	0.095	0.0836	0.3	0.05813	2.8
B2-2	Zr-4 AFA2G (A31)	924.3	926.39	2.09	35.96	0.095	0.0836	0.3	0.05813	2.5
B2-3	Zr-4 AFA2G (AA)	932.7	935.06	2.36	40.6	0.095	0.0836	0.3	0.05813	2.8
B2-4	Zr-4 AFA2G (A43)	903	905.6	2.6	44.73	0.095	0.0836	0.3	0.05813	3.1
C1-1	SRA Low-Sn Zr-4	973.9	976.81	2.91	50.06	0.095	0.0836	0.3	0.05813	3.4
C1-2	PRXA Low-Sn Zr-4	973.6	977.15	3.55	61.07	0.095	0.0836	0.3	0.05813	4.2
C1-3	M5(M5)	1036.9	1039.24	2.34	40.15	0.095	0.0825	0.3	0.05828	2.7
C1-4	Zr-4 AFA2G (--)	904.8	909.14	4.34	74.66	0.095	0.0836	0.3	0.05813	5.1
C2-1	Zr-4 (GTT)	1874.9	1879.79	4.89	63.53	0.124	0.1011	0.3	0.07697	4.3
C2-2	Zr-4 (GTT)	1886.3	1891.14	4.84	62.88	0.124	0.1011	0.3	0.07697	4.3
C2-3	M5(MA)	1010.1	1011.98	1.88	32.26	0.095	0.0825	0.3	0.05828	2.2
D1-1	Alloy B	979.4	982.62	3.22	55.4	0.095	0.0836	0.3	0.05813	3.8
D1-2	Alloy C	962.1	965.07	2.97	51.09	0.095	0.0836	0.3	0.05813	3.5
D1-3	SRA Sandvik Alloy	1102.9	1105.95	3.05	51.17	0.097	0.0842	0.3	0.05960	3.5
D1-4	RXA Sandvik Alloy	1113.3	1116.26	2.96	49.66	0.097	0.0842	0.3	0.05960	3.4
D2-1	M5(M26)	985.5	986.72	1.22	20.93	0.095	0.0825	0.3	0.05828	1.4
D2-2	M4(RA)	962.2	964.61	2.41	41.4	0.095	0.083	0.3	0.05821	2.8
D2-3	M4(R28)	959.8	962.1	2.3	39.51	0.095	0.083	0.3	0.05821	2.7
D2-4	M4(M4)	996.3	999.42	3.12	53.6	0.095	0.083	0.3	0.05821	3.7

Table 5. Average Oxide Thicknesses After Second Interim Inspection.

Rod no.	**Segment no.**			
	1	2	3	4
1	34.21	8.34	8.17	7.66
2	33.52	26.99	10.13	8.36
3	34.79	17.75	8.73	6.13